Int. J. Heat Mass Transfer. Vol. 23, pp. 301–309
© Pergamon Press Ltd. 1980. Printed in Great Britain

0017-9310/80/0301-0301 $02.00/0

HEAT TRANSFER TO A PLANE WALL FROM A HEATED, VENTILATED PLANE JET

G. F. MARSTERS
Department of Mechanical Engineering, Queen's University, Kingston, Ontario, Canada K7L 3N6

and

B. HOWKINS
Imperial Oil Ltd., Don Mills, Ontario, Canada

and

E. KORTSCHAK
DuPont of Canada Limited, Coteau-du-Lac, Quebec, Canada

(*Received* 4 *May* 1979 *and in revised form* 2 *July* 1979)

Abstract – An experimental study of the heat transfer characteristics of a 'ventilated' jet attaching to a plane wall has provided data which aid in the understanding of heat transfer processes involved in this flow. Although the boundary conditions at the wall varied in the streamwise direction, an 'effectiveness' can be defined, and the role of the ventilating flow can be understood. Wall temperature distributions and temperature profiles in the flow field are reported.

NOMENCLATURE

- H, dimensionless gap, h/t_p;
- h, distance from wall to nozzle centreline (gap);
- l, span of jet and wall;
- ΔP, pressure difference;
- $\dot{Q}$, heat transfer rate;
- T, temperature;
- t_p, nozzle width;
- x, coordinate along wall in direction of main flow;
- y, spanwise coordinate;
- z, coordinate normal to wall.

Greek symbol

- θ, temperature excess, $T - T_\infty$.

Subscripts

- ∞, reference (ambient) conditions;
- f, fluid state;
- j, jet conditions at nozzle exit plane;
- Noz, nozzle exit plane;
- w, wall conditions.

INTRODUCTION

A PLANE jet, parallel to a plane, but offset from the wall, attaches to the wall; if there is an open gap between the jet and the wall, the arrangement has been termed a ventilated wall jet [1]. Earlier studies by Marsters [1, 2] have identified the main characteristics of a ventilated plane jet issuing parallel to a plane wall. Other studies by Kumada *et al.* [3] and Ayukawa and Shakuchi [4] as well as by Bourque and Newman [5] have dealt with the wall jet issuing from a nozzle offset from, or inclined with respect to, the wall. In these latter cases, secondary flow is not permitted, with the result that a sizeable recirculation region occurs and a stagnation streamline, originating in the jet flow, can be identified. The jet flow 'attaches' to the wall at a downstream location which is dependent upon step height and nozzle pressure ratio.

Interest in these attaching and ventilated flows has been stimulated because they model, approximately, the behaviour of flows which occur in powered high lift devices for STOL aircraft. Upper surface blowing (USB), thrust augmentor arrangements and some configurations of blown flaps consist of jet sheets blowing over adjacent surfaces and exhibiting Coanda-like 'attachment' to these walls.

The ventilated wall jet allows secondary fluid to be entrained between the wall and the jet. True attachment (in the sense that a stagnation streamline can be identified) does not occur. The prototype configuration is sketched in Fig. 1 while the experimental realization is shown in Fig. 2. In practical applications in STOL devices, the primary jet fluid may be hot, either bypass air from the engine compressor, or very

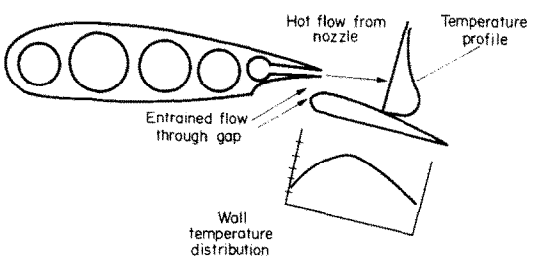

FIG. 1. Possible arrangement of blown, ventilated flap.

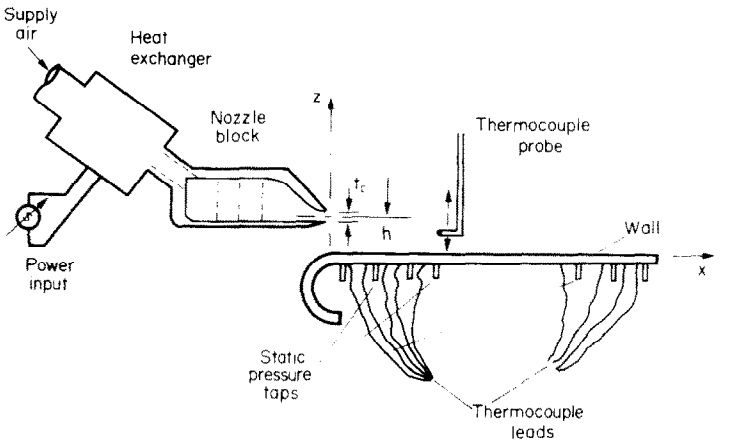

FIG. 2. Schematic diagram of experimental set-up.

hot combustion products from the core flow. Thus it becomes of interest to examine the heat transfer characteristics of such flows and to attempt to establish the 'effectiveness' of heat transfer in the presence of the secondary flow. Although Goldstein [6] has catalogued the heat transfer characteristics of a wide range of geometrical configurations, the ventilated wall jet is absent from the list. The data provided herein constitute a contribution to knowledge about a configuration which, as far as the authors are aware, has not been studied before.

The experiments reported here examined the heat transfer characteristics of a plane ventilated jet of air which was heated. The jet issued from a slot nozzle which was offset from, but parallel to, the plane wall which was instrumented to permit measurement of pressure and temperature along the wall. Traverses of the temperature profile, normal to the wall, were taken at several stations. In addition some observations were made with the secondary flow blocked.

EXPERIMENTAL PROCEDURE

The experimental program made use of an existing apparatus used to study cold ventilated jets. The nozzle block, described in Refs. [1] and [2], was further instrumented with thermocouples in the settling chamber to monitor the supply air temperature. The nozzle dimensions were 2.54 mm (t_p) by 114.3 mm (l). An electrical heating element, taken from a domestic hair dryer, was installed in a 'heat exchanger section' upstream of the nozzle block. The air supply came from an air compressor system which provided a constant supply pressure. The nozzle block and wall (flap*) were mounted between two extensive side walls, thus minimizing spanwise effects and maintaining a high degree of two-dimensionality over most of the flow field.

The flap was fabricated from aluminum, 12.7 mm thick. The plane flap surface was tangent to the constant radius of the curvature leading edge. It was instrumented with 10 pressure taps along the centreline and 10 more at off-centreline locations as shown in Table 1. The off-centreline taps were situated symmetrically with respect to the centreline, at 41 mm from the centreline. The flap also incorporated 33 thermocouples which were located as shown in Table 2. As in the case of the wall pressure taps some thermocouples were located at (symmetrical) positions 41 mm from the centreline. Most of the thermocouples were set in the plate, using 2.38 mm diameter holes drilled from the bottom surface, and were approximately 0.79 mm from the top surface. (The top surface is the surface in contact with the secondary

*The terms 'wall' and 'flap' are used interchangeably in this paper.

Table 1. Pressure tap locations (aft from nozzle exit plane, mm)

Station No.		$\mathcal{L}$	R	Station No.	L	$\mathcal{L}$	R
1		0		11		114.3	
2		38.1		12		139.7	
3	38.1			13	152.4		
4			50.8	14			152.4
5		63.5		15		165.0	
6		76.2		16		200.7	
7			76.2	17	228.6		
8		88.9		18			228.6
9	101.6			19		228.6	
10			101.6	20		279.4	

Table 2. Thermocouple locations (aft from nozzle exit plane, mm)

Station No.	L	$\mathcal{L}$	Station No.	L	$\mathcal{L}$	R
1	95.25		18			95.25
2		57.15	19			95.25B
3		69.85	20			114.3
4		69.85B	21			114.3B
5		82.55	22		133.35	
6		95.25	23		146.05	
7		95.25B	24		158.75	
8		107.95	25			158.75
9		114.3	26		184.15	
10		114.3B	27		184.15B	
11	158.75		28			234.95
12	114.3B		29		304.8	
13	114.3		30		304.8B	
14	234.95		31	95.25B		
15		234.95	32		12.7	
16		44.45	33		12.7B	
17		44.45B				

Note: Symbol 'B' denotes thermocouple located near bottom surface of flap.

flow). Several thermocouples were situated approximately 1.0 mm from the bottom surface, to assist in determining the extent of heat conduction through the flap from top to bottom. The flap had 6.35 mm thick plexiglass 'end walls' attached to reduce spanwise conduction. Because of the thickness of the flap, an adiabatic surface was not attained. The heat transfer from the jet resulted in a maximum temperature near (but downstream of) the point of maximum pressure on the flap surface, with a rather steep temperature gradient upstream of the maximum. This gave rise to conduction along the flap in the upstream direction. Although this effect could have been avoided by using a thin metallic film for the upper surface, bonded to a material of low conductivity, other disadvantages, for example, the increased difficulty in obtaining static pressure distribution, lead to the construction shown in Fig. 3. Figure 3 shows some of the details of the arrangement, and includes some of the nomenclature used. The use of a 'film' surface is discussed later.

All thermocouples were copper–constantan, which were connected, by means of a multipoint switch, to a reference junction in an ice–water bath, and the outputs were recorded on a chart recording potentiometer capable of reading 5 mV full scale. The thermocouple used to obtain temperatures in the jet flow field was also copper–constantan with a bead approximately 0.46 mm diameter. The maximum temperature excesses in the jet, θ_j, were never more than 35°C.

The wall static pressure taps were connected to a tilting multitube manometer bank. The jet velocity was observed by means of a total head tube ($\simeq$ 1.3 mm OD) situated within one slot width of the nozzle exit plane, inside the potential core of the jet flow. Nominal jet velocities of 80 m s^{-1} were used, and incompressible flow has been assumed throughout. This velocity yields a nominal Reynolds number, based on slot width, t_p, of 7100. Although the two-dimensionality of the flow is difficult to preserve at downstream stations,

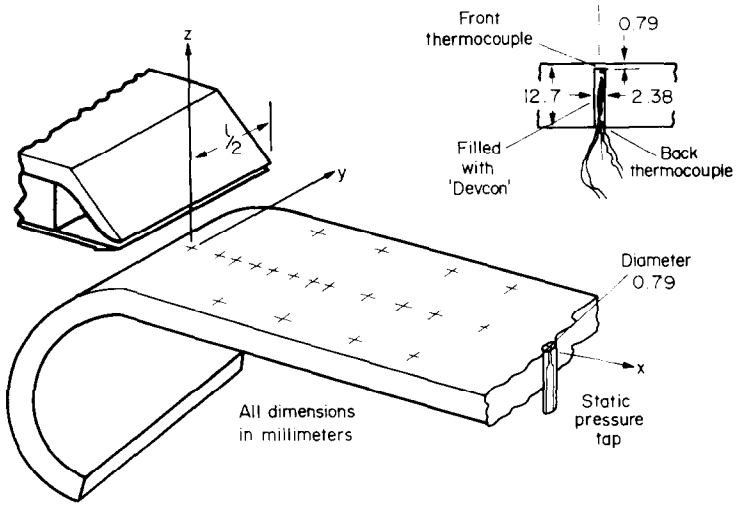

FIG. 3. Schematic of wall/nozzle arrangement showing some details of instrumentation.

earlier studies [1, 2] along with the present measurements of the temperature and pressures suggest that a fairly high degree of two-dimensionality is maintained in the regions of interest.

Experiments on this apparatus required fairly long periods of time to achieve a steady state for the wall temperature distribution. Initially, steady flow conditions, at the correct nozzle velocity must be established, following which the temperature of the flow was adjusted to the desired level by means of a Variac controlling the electrical power to the air heater. After this was achieved, approximately 2 h were required to achieve steady wall temperatures. Observation of the top and bottom surface of the flap showed that conduction in the direction normal to the flap surface was generally negligible, as was spanwise conduction. The effects of streamwise conduction will be discussed later.

Because the flap was neither isothermal nor adiabatic, the final temperature distribution is somewhat dependent upon the geometry used and the nature of the surroundings. In particular, streamwise conduction in the flap results in a 'smearing' of the temperature distribution. It is of interest to check on the temperature distribution for the case where streamwise conduction is negligible.* To do this a surface consisting of a thin (0.102 mm) aluminum film was bonded to a plexiglass wall, 25.4 mm thick. Thermocouples were fed from the back surface and placed in small indentations in the plexiglass before the foil was attached. Care was taken to ensure that there was good contact between the foil and the thermocouples. For this arrangement, streamwise conduction along the foil was negligible and for very short observation times ($\simeq$ 10 s) the surface was approximately adiabatic. Experiments were conducted as follows. A styrofoam sheet was used to insulate the wall from the jet while the jet temperature was stabilized. Then the styrofoam was removed as quickly as possible (a few milliseconds) and the wall thermocouples were scanned rapidly. The resulting distribution is shown along with the 'steady state' results.

PRESENTATION OF RESULTS

Experiments were conducted with several different gaps, h, between the flap surface and the jet centreline, for the ventilated case, but for space reasons only representative data will be reported here. Two sets of data were obtained for the case of the offset jet with no secondary flow, at two values of h. Temperature profiles in the flow field were also obtained.

Wall static pressures

The distribution of wall static pressures, in the form of a pressure coefficient multiplied by the dimensionless offset distance, H ($= h/t_p$), is plotted versus dimensionless downstream distance. The results for two ventilated cases are shown in Fig. 4. A cross-hatched region, representing the data obtained by Marsters [1] is superimposed on the figure. Although this experiment uses a different flap, with a modified leading edge, it is clear that the main characteristics of the flow are the same as found in the earlier work. The pressure distribution for the case of the blocked secondary flow at $H = 11.75$, which illustrates rather dramatically the steep pressure gradients encountered in these recirculating flow, is shown in Fig. 5. All these pressure distribution data are in good agreement with past experience. In view of this agreement, no measurements of velocity distributions were undertaken. In addition, the off-axis pressure taps showed only small

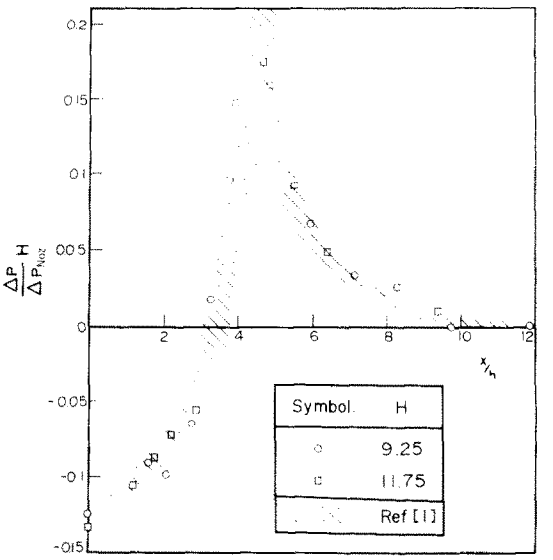

FIG. 4. Wall static pressure distributions for ventilated flow. Shaded area corresponds to data from Ref. [1].

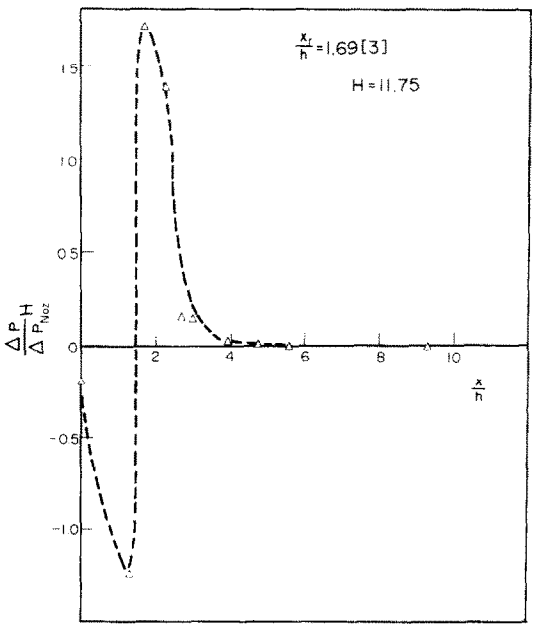

FIG. 5. Wall static pressure distribution, blocked secondary flow. x_r/h calculated from relationship in Ref. [3].

*This experiment was suggested by one of the reviewers.

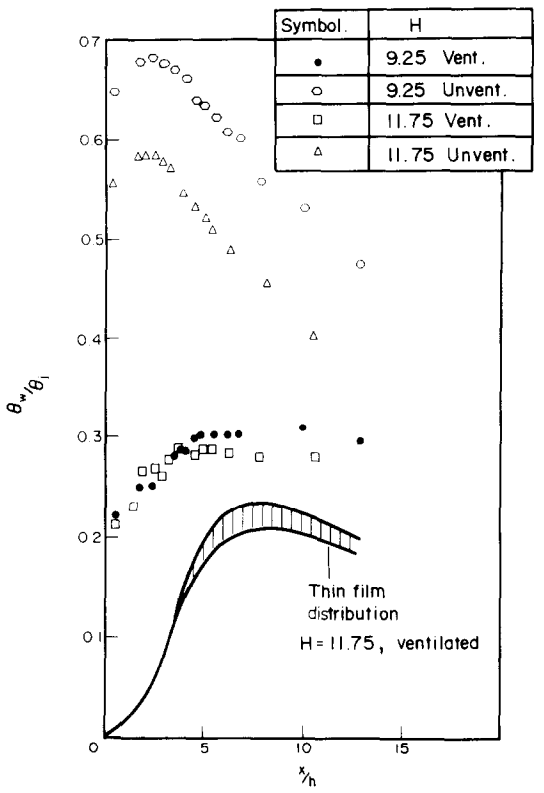

FIG. 6. Wall temperature distributions for four cases. Temperatures measured using thermocouples on centreline, near top surface of wall.

differences from the centreline values, confirming that large departures from two-dimensionality were unlikely to occur.

Wall temperatures

The centreline excess temperatures at the wall, θ_w, normalized with respect to the jet excess temperature, θ_j, is defined as the 'effectiveness' of heat transfer for this flow. This quantity is plotted vs dimensionless distance downstream for two gaps in Fig. 6. We first consider the ventilated flow cases. Comparing these distributions with the wall pressure distributions shows that the temperature rises and reaches a 'plateau' near the point at which static pressure is a maximum. Just as in the case of the pressure distributions, steep gradients occur upstream of the maximum values. However, the temperature distribution does not return to ambient downstream, and as a result there is a net heat flux at the trailing edge of the flap. Upstream of the maximum temperature there is a significant heat flux in the upstream direction. The relative magnitude of this heat flux will be evaluated in the discussion section following.

The results for the 'thin film' experiment are shown in Fig. 6 as a cross-hatched band. The results show much steeper temperature gradients, as would be expected. Because the film was not perfectly adiabatic, the maximum temperature did not rise to the level of the steady state experiments. The plexiglass substrate temperature would rise very slowly via conduction normal to the plate, and after a very long time, a distribution comparable to that for the aluminum flap would be achieved. These results were obtained at very early times (because of finite conduction there are transient effects) and are presented to show the approximate shape of the distribution curve which would obtain in a perfectly adiabatic wall. Although the inherent error in the 'film' data is fairly significant, the differences between the case of axial conduction and no axial conduction are clearly evident.

Turning attention now to the unventilated case, also shown in Fig. 6, it is found that the plate temperature excess is higher and has shifted well upstream. The gradient is also very steep. The temperature distribution reflects the flow pattern which may be inferred from the pressure plot for this case. In this flow field there is a stagnation streamline and some of the hot jet fluid actually moves upstream in the recirculation bubble, along the flap surface. As a result the temperature of the recirculating fluid will be quite high.

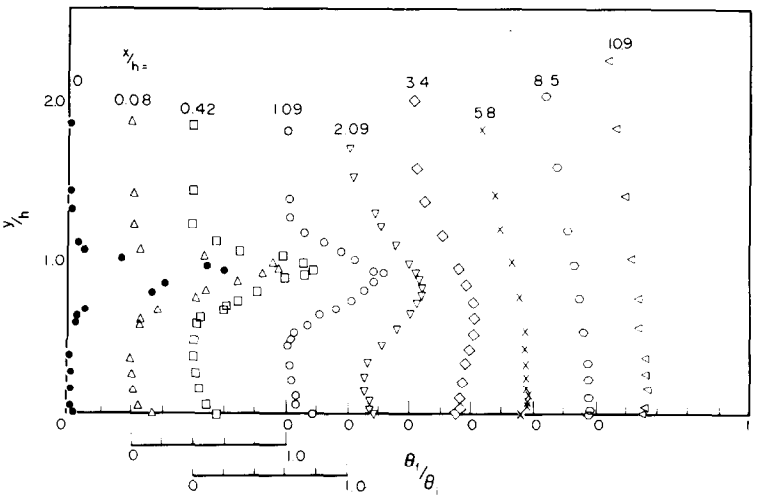

FIG. 7. Temperature profiles observed in fluid along wall centreline. Ventilated case, $H = 11.75$.

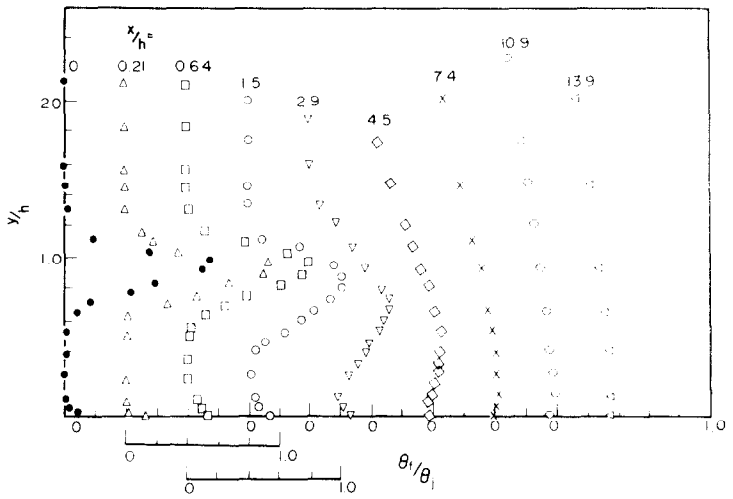

FIG. 8. Temperature profiles observed in fluid along wall centreline. Ventilated case, $H = 9.25$.

Moreover, there are fairly strong temperature gradients of opposite sign downstream of the peak temperature. Conduction along the plate is thus seen to be important in this case.

Temperature distributions in the flow

A small thermocouple probe was traversed through the flow normal to the flap surface. These traverses could be carried out at any downstream station. The thermocouple output was recorded using a chart-recording potentiometer. The streamwise stations at which these mid-span traverses were conducted were chosen on the basis of the wall pressure and temperature data just presented.

Fluid temperature distributions, again presented as local excess temperature, θ_f, normalized with θ_j, are shown in Figs. 7 and 8 for jet-to-wall spacings of 11.75 and 9.25 respectively. The temperature profiles for the blocked secondary cases are shown in Figs. 9 and 10. These plots should be examined along with the comparable plots of wall temperature distribution. The parameter, x/h, is the downstream distance from the nozzle exit plane. Notice that the station $x/h = 0$ is 12.7 mm upstream of the first thermocouple (No. 32, Table 2).

Dealing with the largest gap first, the profiles nearest the nozzle show, as the wall is approached from large values of y/h, a well-defined hot jet, followed by ambient temperatures in the secondary flow. The temperature rises again from approximately ambient temperatures very near the flap surface. This indicates heat transfer from the wall to the secondary stream. At stations near the point of maximum wall temperature, the temperature gradient adjacent to the wall is essentially zero, although a maximum temperature is observed at some distance from the wall.

In Fig. 8 we see approximately the same sort of distribution. The slight differences in the temperature distributions along the wall are accompanied by slightly modified temperature distributions in the fluid. Nonetheless, the temperature gradient in the fluid near the wall show a reversal of temperature

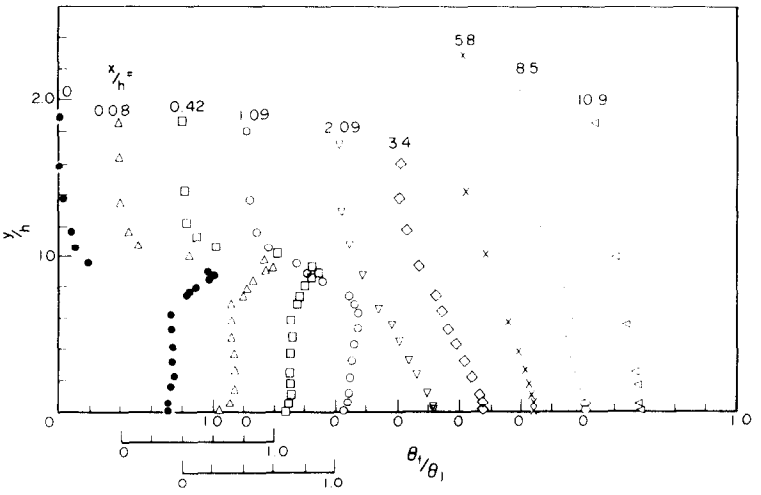

FIG. 9. Temperature profiles observed in fluid along wall centreline. Blocked secondary flow, $H = 11.75$ (unventilated).

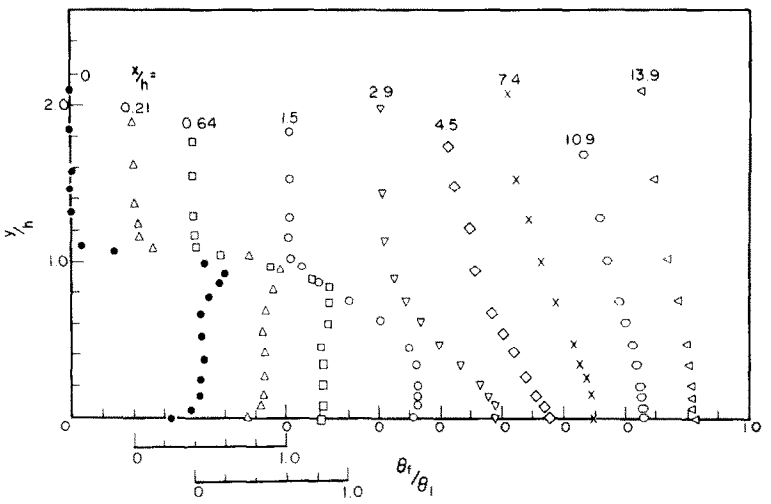

FIG. 10. Temperature profiles observed in fluid along wall centreline. Blocked secondary flow, $H = 9.25$ (unventilated).

gradient in the fluid indicating a reversal of direction of heat flux near the point where the wall temperature reaches the plateau. The main features of the temperature profiles in the fluid are reproduced for each gap setting.

The case of the blocked secondary flow, Figs. 9 and 10, is quite different, as one might expect from the distributions of wall temperatures. The outer flow exhibits the same features as for the other cases, but the inner flow is changed rather significantly, with temperatures in the fluid greater than or equal to the wall temperature. Thus the heat flux is from the fluid to the wall over virtually all of the surface. Also, the temperature excess is generally greater than in the case of the ventilated flow.

Plots showing the isotherms as determined from these traverses are shown in Figs. 11 and 12. These illustrate the temperature distributions in the fluid and suggest the directions of heat flux at the wall.

DISCUSSION

Examinations of the wall temperature excess or the fluid temperature distributions indicate that the effectiveness of a ventilated jet is decreased as the gap is increased. This is to be expected, of course, since the secondary flow provides an insulating blanket of fluid next to the wall, thus reducing heat flux rates to the wall. In addition, the secondary stream provides an additional mass of fluid which mixes with the primary stream, producing a more rapid decrease in the maximum temperature in the downstream direction. The trajectory of the maximum fluid temperature is shown in Fig. 13.

Returning to the wall temperature excess, the conduction along the wall is seen to be important where axial gradients are steep, i.e. upstream of the point of maximum wall temperature. Because of these relatively high fluxes, heat is transferred along the wall upstream, and thence to the secondary stream. The

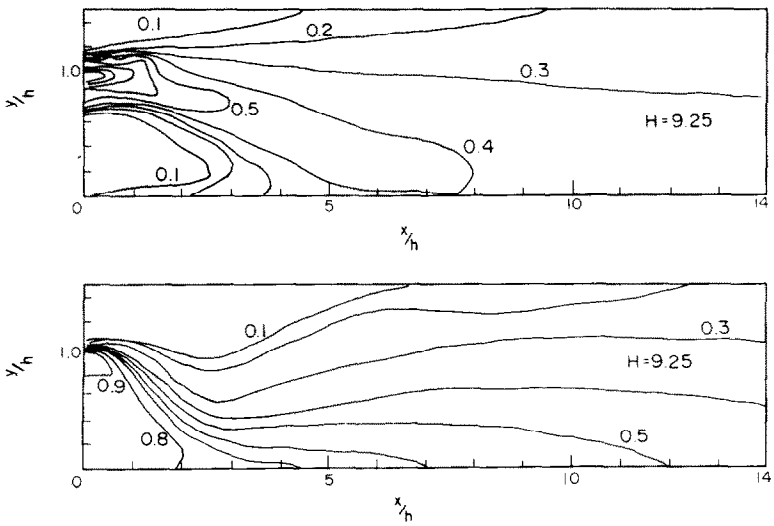

FIG. 11. Isotherms in fluid, in terms of temperature excess θ_f/θ_j. Top, ventilated; bottom, blocked secondary; $H = 9.25$.

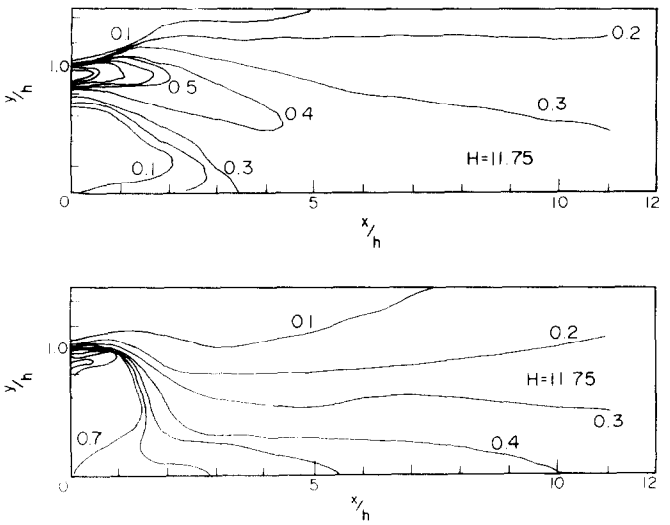

FIG. 12. Isotherms in fluid, in terms of temperature excess, θ_f/θ_j. Top, ventilated; bottom, blocked secondary; $H = 11.75$.

fluid temperature profiles show this clearly, exhibiting negative values of $\partial T/\partial y$. The maximum rate of axial heat flux, $\dot{Q}$, for a ventilated wall is roughly constant for x/h less than 4 for $H = 9.25$. This rate is estimated to be about 3 W. The total heat addition rate for the jet was approximately 1 kW. Thus, the axial conduction is small compared to the total energy introduced into the jet fluid, but less than half of this total energy is available for transfer to the wall, since the outer side of the jet mixes freely with the surroundings. The wall temperature gradients downstream of the maximum wall temperature are negligible, hence, one concludes that axial conduction in the streamwise direction is negligible. Also, data obtained in this study show that conduction through the flap from top to bottom is negligible; the same is also true for spanwise conduction.

The situation in the case of the blocked secondary flow deserves special attention. Here again we see steep streamwise temperature gradients in the wall, which yield conduction heat fluxes comparable to those encountered in the ventilated case. Despite this streamwise conduction, the fluid temperature profiles suggest heat transfer from the fluid to the wall in the recirculating bubble region. As mentioned earlier, these profiles reveal a peak temperature through the jet, then an elevated temperature in the recirculation region, and a rather sharp decrease in temperature adjacent to the flap surface. This is easily explained as follows. The 'stagnation streamline' springs from the interior of the jet at the nozzle, not the nozzle lip. Thus, some of the hot jet fluid, only slightly cooled by mixing with fluid in the recirculating bubble, moves 'upstream' from the stagnation point. This constitutes a hot 'wall jet' moving upstream from the stagnation point as well as downstream. Despite axial conduction, the steady state is one where the wall is always cooler

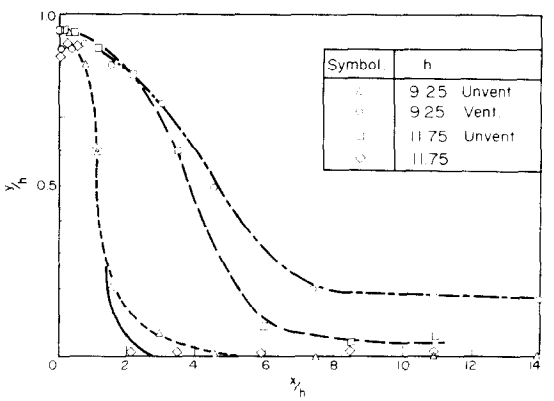

FIG. 13. Trajectories of maximum centreline temperature for two gap settings and both open and blocked secondary flows.

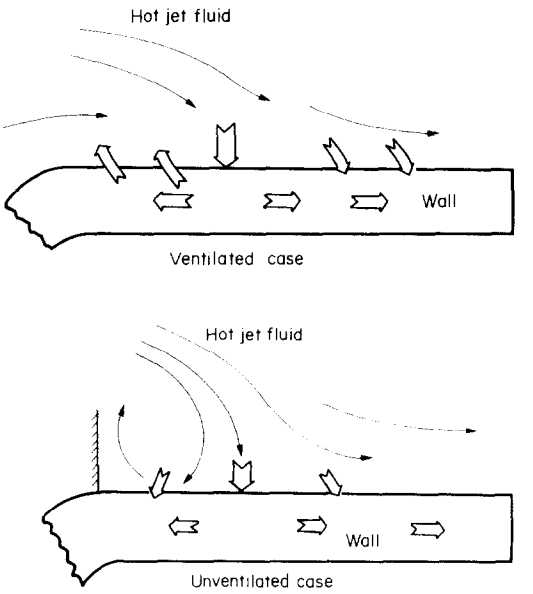

FIG. 14. Schematic diagram showing heat flux directions for the ventilated and unventilated flows.

than this wall jet. These heat fluxes are shown schematically in Fig. 14.

SUMMARY AND CONCLUSIONS

This study has presented new heat transfer data on a configuration termed a ventilated wall jet, wherein the jet fluid was heated. The resultant wall temperature distribution, due to the transfer of heat from the jet, has been mapped in detail for two different offset gap values. The temperature distribution in the primary and secondary flows have also been surveyed, along with the wall static pressure distribution. The case where the secondary flow is blocked by a solid wall has been examined as well, and data for wall temperature distributions, and wall static pressures have been presented also. This special case is compared with the ventilated flow cases, and the differences discussed.

Acknowledgement — This work has been partially supported by Grant No. A4310 from the National Research Council of Canada.

REFERENCES

1. G. F. Marsters, The attachment of a plane ventilated jet to a plane parallel wall, *CSME Trans.* **4,** 197–202 (1976/77).
2. G. F. Marsters, The attachment of a ventilated plane jet to an inclined plane wall, *Aero. Quart.* **29,** 60–74 (1978).
3. M. Kumada, I. Mabuchi and K. Oyakawa, Studies on heat transfer to turbulent jets with adjacent boundaries, 3rd Report, *Bull. JSME* **16,** 1712–1722 (1973).
4. K. Ayukawa and T. Shakouchi, Analysis of a jet attaching to an offset parallel plate, 1st Report, *Bull. JSME* **19,** 395–401 (1976).
5. C. Bourque and B. G. Newman, Reattachment of a two-dimensional incompressible jet to an adjacent flat plate, *Aero. Quart.* **11,** 201–232 (1960).
6. R. J. Goldstein, Film cooling, in *Advances in Heat Transfer*, Vol. 7, pp. 321–379. Academic Press, New York (1971).

TRANSFERT THERMIQUE ENTRE UNE PAROI PLANE ET UN JET PLAN CHAUD

Résumé – Une étude expérimentale du transfert de chaleur d'un jet soufflé sur une paroi plane a donné des résultats qui aident la compréhension des mécanismes présents dans cet écoulement. Bien que la condition limite sur la paroi varie dans la direction de l'écoulement, une efficacité peut être définie et le rôle du soufflage peut être compris. On donne des profils de température et des distributions de température pariétale.

WÄRMEÜBERGANG AN EINE EBENE WAND VON EINEM BEHEIZTEN, BELÜFTETEN EBENEN FREISTRAHL

Zusammenfassung – Eine experimentelle Untersuchung der Wärmeübertragungs-Kenngrößen eines 'belüfteten' Freistrahls, der an einer ebenen Wand anliegt, hat Ergebnisse geliefert, die für das Verständnis der Wärmeübertragungs-Prozesse, die bei dieser Strömung auftreten, hilfreich sind. Obwohl sich die Grenzschichtbedingungen an der Wand in Strömungsrichtung ändern, kann ein Wirkungsgrad definiert werden, und die Rolle der Belüftungs-Strömung wird verständlich. Es werden Temperaturverteilungen und Profile in dem Strömungsfeld angegeben.

ТЕПЛОПЕРЕНОС К СТЕНКЕ ПРИ ЕЁ ОБДУВЕ ПЛОСКОЙ СТРУЁЙ

Аннотация — Из опытов по теплообмену струи, омывающей плоскую стенку, получены данные, способствующие пониманию процессов теплопереноса для течения такого типа. Несмотря на переменность граничных условий вдоль стенки, можно определить «эффективность» процесса и оценить роль обдува. Даны распределения температур стенки и профили температур в пристенном потоке.